

Self-Consistent-Field Prediction for the Persistence Length of Wormlike Micelles of Nonionic Surfactants

Yansen Lauw,* Frans A. M. Leermakers, and Martien A. Cohen Stuart

Laboratory of Physical Chemistry and Colloid Science, Wageningen University,
Dreijenplein 6, Wageningen 6700 EK, The Netherlands

Received: May 28, 2003; In Final Form: August 5, 2003

The persistence length of wormlike micelles is predicted using a molecular realistic self-consistent-field theory by analyzing the curvature energy stored in toroidal micelles. It is assumed that the growth of the torus is unidimensional and its cross section is a perfect circle with radius of the torus R_t and curvature $J = 1/R_t$. For C_nE_m nonionic surfactants, it is found that the persistence length l_p scales with respect to the tail group length n as $l_p \sim n^x$ where x is about 2.4–2.9. For sufficiently long hydrophobic tail length, the wormlike micelles become more rigid with increasing temperature and for short-tail surfactants, the reverse is found. Remarkably, curvatures in the order of the inverse persistence length are such that J^4 and J^6 terms are needed to know the bending energy for this case. This effect is more pronounced the larger the head and the smaller the tail group.

1. Introduction

The study of wormlike micelles has intensified in recent years.^{1–3} Wormlike micelles are examples of living (reversible) polymers. One important parameter that characterizes these micelles is their persistence length l_p . In this article, self-consistent-field theory (SCF) is used to evaluate the bending free energy of a closed wormlike micelle (torus) that consists of nonionic surfactants in aqueous solutions. From this, it is possible to evaluate the persistence length of the micelles.

Surfactants can form micelles beyond a particular concentration. The concentration at which micelles start to form is generally known as the critical micellization concentration (CMC). Micelles can be found in various topologies. There exists a governing packing parameter P which is defined as the ratio of the volume of the tail (hydrophobic) group with the product of the head (hydrophilic) group area and the length of the tail group, such that for spherical micelles $P \leq 1/3$, for cylindrical micelles $1/3 < P \leq 1/2$, and planar bilayers $1/2 < P \leq 1$. The transition from spherical to cylindrical micelles is through the toroidal shapes with increasing surfactant concentration.⁴ Below, we employ an SCF analysis and impose in all cases a toroidal geometry onto the surfactant aggregates, irrespective of the true value of the surfactant packing parameter. By doing so, we can systematically investigate the influence of different surfactant architectures on the persistence length. We return to this computational constraint in the discussion.

The persistence length of a wormlike micelle l_p is defined as the length over which the correlation of directional orientation along the contour of the micelle is reduced by a factor e . Generally, the persistence length l_p is thus the distance along the contour of the micelle up to which it can be considered as a rigid rod. In other words, a cylindrical micelle with a length $l < l_p$ behaves nearly as a rod, whereas one with a length $l > l_p$ can be considered as a flexible cylindrical micelle.⁵ Common examples of a wormlike micelle are found in ionic surfactants such as cetyltrimethylammonium bromide (CTAB), cetylpyridinium (CP) bromide, or CP chlorate with added salt;^{6–8} nonionic surfactant like hexaethylene glycol monohexadecyl

ether ($C_{16}E_6$);⁹ and in the mixed solution of bile salt and phosphatidylcholine (PC).¹⁰

The toroidal shape of micelles is experimentally observed for gemini surfactants,^{11,12} the ionic surfactant cetyltrimethylammonium chloride (CTAC) with added salicylate,¹³ and the nonionic surfactant $C_{16}E_6$ in D_2O with and without added salt.⁹ Charged surfactants are considerably more difficult to model than nonionic ones. For this reason, we select nonionic surfactants for the present first attempt to predict trends in l_p .

The relation between the persistence length of a cylindrical micelle and its bending modulus κ is¹⁴

$$l_p = \frac{\kappa}{k_B T} \quad (1)$$

where T is the absolute temperature and k_B the Boltzmann constant. In this article, l_p is made dimensionless by normalizing it with a characteristic length a which is equal to the size of a lattice site. Details about the discretization scheme of the surfactant molecules are discussed in section 2 of this paper.

In 1973, Helfrich¹⁵ derived a general relation between the surface tension γ and bending parameters of self-assembled surfactant (bi)layers in which the total and Gaussian curvatures are the two governing variables. For a wormlike micelle, it suffices to express surface tension solely as a function of its curvature J . The Gaussian curvature vanishes since only one radial variable is needed to describe the shape of linear micelles. Therefore, the Helfrich expression for a wormlike micelle is

$$\gamma(J) = \gamma(0) - \kappa J_0 J + \frac{1}{2} \kappa J^2 \quad (2)$$

where $\gamma(0)$ is the surface tension for zero curvature, κ the bending modulus, and J_0 the spontaneous curvature, i.e., the curvature in equilibrium assumed by an unconstrained wormlike micelle.

To evaluate the bending rigidity of wormlike micelles, it is convenient to consider homogeneously curved cylindrical micelles. Such micelles assume the toroidal shape (see Figure 1). Toroidal micelles are cylindrical micelles that have no ends.

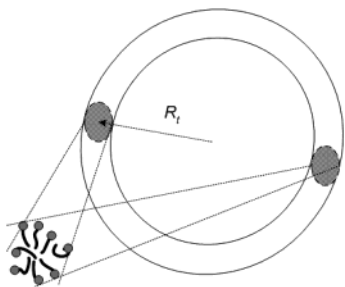


Figure 1. Illustration of a toroidal micelle and its cross section. The radius of the torus is denoted by R_t .

The primary quantity of interest is the grand potential Ω of the toroidal micelle as a function of $J = 1/R_t$, where R_t is the toroidal radius (see Figure 1). The grand potential Ω is identified as the bending energy of the torus. Realizing that $\gamma(0)$ and J_0 are equal to zero (the uncurved micelle is tensionless and has no preferred curvature), eq 2 may be rewritten as

$$\gamma(J) = \frac{\Omega}{l} = \frac{1}{2} \kappa J^2 \quad (3)$$

By substituting the length of the torus $l = 2\pi R_t = 2\pi/J$ into eq 3, the bending energy of the torus turns out to be $\Omega = \pi \kappa J$. Note that this expression is accurate only for small values of J . Equation 3 can be written more conveniently in terms of the persistence length stated in eq 1:

$$\Omega = \pi l_p k_B T J \quad (4)$$

2. Self-Consistent-Field Theory

The bending energy Ω is numerically accessible in a self-consistent-field theory. Here such theory is used by implementing the discretization scheme due to Scheutjens and Fleer.^{16–22} To determine the statistical weight of various conformations of surfactants, the molecules are considered to be composed of segments. A sequence of segments defines the architecture of the surfactants. Space is discretized by using a lattice. Each segment just fits one lattice site with characteristic size a . The characteristic dimension of a lattice site is used to make all distances dimensionless. It is essential to know that in this lattice system there exist layers of lattice sites in which the density of molecular components is assumed to be homogeneous and that gradients in density can develop between different layers. To describe the torus, the use of a cylindrical coordinate system is necessary (Figure 2).

Referring to Figure 2, z denotes the orthogonal layer number which runs from $z = -M_z$ to M_z . The radial layer number r goes from $r = 0$ to M_r ; $r = 0$ is the center of the torus. M_r is taken large enough to ensure that the last layers are in the bulk phase. All lattice sites that have the same (z, r) coordinates will have the same volume fraction of segments (mean-field approximation). For this reason it is possible to map the 3-dimensional system onto a 2-dimensional grid as can be seen at the right-hand side of Figure 2.

In the SCF method, the statistical weight of segments of type A in layer (z, r) is expressed in a segment-weighting factor $G_A(z, r)$ which is defined as

$$G_A(z, r) = \begin{cases} \exp\left\{\frac{-u_A(z, r)}{k_B T}\right\} & , \quad 0 < z < z_{\text{bulk}}, \quad 0 < r < r_{\text{bulk}} \\ 1 & , \quad z \geq z_{\text{bulk}}, \quad r \geq r_{\text{bulk}} \end{cases} \quad (5)$$

The mean-field assumption allows for a single value of $G_A(z, r)$ for all segment types A and all positions in layer (z, r) . The potential energy of the segment A, $u_A(z, r)$, sometimes referred to as the self-consistent potential, is also homogeneous for all sites with the same (z, r) coordinate. In expression 5, z_{bulk} is the layer where the bulk phase is reached, i.e., at least in the last layer. Furthermore, the self-consistent potential depends on the volume fraction of each segment type in layer (z, r) and features the well-known Flory–Huggins interaction parameter χ that parametrizes short-range nearest-neighbor interactions,

$$u_A(z, r) = u'(z, r) + k_B T \sum_B \chi_{AB} (\langle \phi_B(z, r) \rangle - \phi_B^b) \quad (6)$$

The contribution $u'(z, r)$ is the potential energy required to guarantee that in each layer all lattice sites are occupied by segments (incompressibility constraint). In eq 6, χ_{AB} is the Flory–Huggins interaction parameter between segment types A and B; $\phi_B(z, r)$ is the volume fraction of segment type B in layer (z, r) . The angular brackets indicate that the quantity is averaged over neighboring layers of (z, r) . The notation ϕ_B^b refers to the volume fraction of segment type B in the bulk phase. The averaged volume fraction can be written in the continuous form, which in the case of cylindrical coordinate system is given by

$$\langle \phi_B(z, r) \rangle \approx \phi_B(z, r) + \frac{1}{3} \frac{1}{r} \frac{\partial \phi_B(z, r)}{\partial r} + \frac{1}{3} \frac{\partial^2 \phi_B(z, r)}{\partial r^2} + \frac{1}{3} \frac{\partial^2 \phi_B(z, r)}{\partial z^2} \quad (7)$$

The discrete form of this equation, which is needed in the context of the discrete lattice model, is obtained by applying different bond-weighting factors $\lambda_{-1}(r)$, $\lambda_0(r)$, and $\lambda_1(r)$ to the volume fractions at neighboring sites,

$$\begin{aligned} \langle \phi_B(z, r) \rangle = & \frac{1}{3} \lambda_{-1}(r) \{ \phi_B(z-1, r-1) + \phi_B(z, r-1) + \phi_B(z+1, r-1) \} \\ & + \frac{1}{3} \lambda_0(r) \{ \phi_B(z-1, r) + \phi_B(z, r) + \phi_B(z+1, r) \} \\ & + \frac{1}{3} \lambda_1(r) \{ \phi_B(z-1, r+1) + \phi_B(z, r+1) + \phi_B(z+1, r+1) \} \end{aligned} \quad (8)$$

under the constraint $\lambda_{-1}(r) + \lambda_0(r) + \lambda_1(r) = 1$, $\forall r \in [1, M_r]$.

In the cylindrical coordinate system, $\lambda_{-1}(r)$, $\lambda_1(r)$, and $\lambda_0(r)$ are a priori step probabilities²²

$$\begin{aligned} \lambda_{-1}(r) &= \lambda \frac{S(r-1)}{L(r)} \\ \lambda_1(r) &= \lambda \frac{S(r)}{L(r)} \\ \lambda_0(r) &= 1 - \lambda_{-1}(r) - \lambda_1(r) \end{aligned} \quad (9)$$

where $S(r)$ is the contact area in the radial direction between layers r and $(r+1)$ per unit orthogonal layer. In the cylindrical lattice, $S(r) = 2\pi r$ and the number of lattice sites $L(r)$ in layer r is given by $L(r) = \pi(2r-1)$. Both $S(r)$ and $L(r)$ are invariant in the orthogonal direction. The quantity λ is the one-dimensional bond-weighting factor which depends on the geometry of the equivalent planar lattice. In our calculations $\lambda = 1/3$ is used throughout.

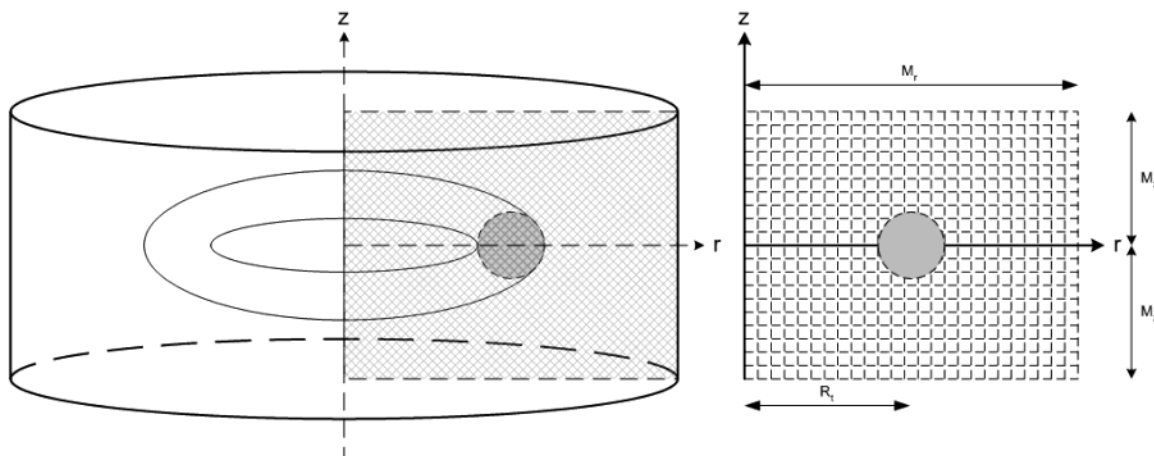


Figure 2. Discretization of space in a lattice model using a cylindrical coordinate system. The orthogonal coordinate is represented by z and the radial by r . The three-dimensional representation of the model is depicted on the left and the cross section is on the right. The radius of the torus is denoted by R_t .

Quantities that depend on the segment type, $u_A(z, r)$, $G_A(z, r)$ and $\phi_A(z, r)$ can be generalized to quantities that depend on the type of molecule i and segment ranking number s in the molecule. By introducing the chain architecture operator $\delta_{i,s}^A$ with property $\delta_{i,s}^A = 1$ when segment s of molecule i is of type A and zero otherwise, one can write

$$u_i(z, r, s) = \sum_A u_A(z, r) \delta_{i,s}^A \quad (10a)$$

$$G_i(z, r, s) = \sum_A G_A(z, r) \delta_{i,s}^A \quad (10b)$$

$$\phi_A(z, r) = \sum_i \sum_s \phi_i(z, r, s) \delta_{i,s}^A \quad (10c)$$

The segment weighting factors are used to analyze the statistical weight of the complete set of all possible conformations of the chainlike surfactants. This overall statistical weight is easily calculated using a Markov approximation. To do this, it is convenient to introduce the chain segment weighting factor $G_i(z, r, s | 1)$ for segment s of molecule i at coordinate (z, r) connected by $s - 1$ segments to segment $s = 1$. In continuous form this quantity can be found by solving the diffusion equation,

$$\frac{\partial G_i(z, r, s | 1)}{\partial s} = \frac{1}{3} \frac{1}{r} \frac{\partial G_i(z, r, s | 1)}{\partial r} + \frac{1}{3} \frac{\partial^2 G_i(z, r, s | 1)}{\partial r^2} + \frac{1}{3} \frac{\partial^2 G_i(z, r, s | 1)}{\partial z^2} - \frac{u_i(z, r, s)}{k_B T} G_i(z, r, s | 1) \quad (11)$$

In the discrete form, the chain segment weighting factors $G_i(z, r, s | 1)$ are calculated by a propagator formalism

$$G_i(z, r, s | 1) = \begin{cases} G_i(z, r, 1) & , s = 1 \\ \langle G_i(z, r, s - 1 | 1) \rangle G_i(z, r, s) & , s > 1 \end{cases} \quad (12)$$

where the average chain segment weighting factor $\langle G_i(z, r, s - 1 | 1) \rangle$ is analogous to the average volume fraction, weighted by the bond-weighting factors

$$\begin{aligned} \langle G_i(z, r, s - 1 | 1) \rangle = & \frac{1}{3} \lambda_{-1}(r) \{ G_i(z - 1, r - 1, s - 1 | 1) + G_i(z, r - 1, s - 1 | 1) \\ & + G_i(z + 1, r - 1, s - 1 | 1) \} \\ & + \frac{1}{3} \lambda_0(r) \{ G_i(z - 1, r, s - 1 | 1) + G_i(z, r, s - 1 | 1) \\ & + G_i(z + 1, r, s - 1 | 1) \} \\ & + \frac{1}{3} \lambda_1(r) \{ G_i(z - 1, r + 1, s - 1 | 1) + G_i(z, r + 1, s - 1 | 1) \\ & + G_i(z + 1, r + 1, s - 1 | 1) \} \end{aligned} \quad (13)$$

The complementary chain segment weighting factor $G_i(z, r, s | N)$, i.e., the quantity that is proportional to the probability of finding a chain fragment from the last segment N_i to s such that segment s of molecule i is at (z, r) , is evaluated using complementary eqs 12 and 13. When all segment weighting factors are known, the volume fraction of segment s of molecule i is obtained from the composition law

$$\phi_i(z, r, s) = C_i \frac{G_i(z, r, s | 1) G_i(z, r, s | N)}{G_i(z, r, s)} \quad (14)$$

where C_i is a normalization factor which, for a grand canonical ensemble (ϕ_i^b fixed), is stated as $C_i = \phi_i^b / N_i$. Alternatively, C_i depends on the number of molecules n_i of type i in the system such that $C_i = n_i / G_i(1 | N)$, where $G_i(1 | N) = \sum_z \sum_r L(r) G_i(z, r, 1 | N)$. By using eq 10c the volume fraction of each segment type can be found and eq 6 can be evaluated via eq 8. An important condition that has to be satisfied is $\sum_A \phi_A(z, r) = 1$ for all layers (z, r) . This is also known as the packing (incompressibility) constraint which determines the values of $u^*(z, r)$. The set of equations is thus closed. To find solutions, an iterative procedure must be applied to obtain all potentials $u_A(z, r)$ and segment volume fractions $\phi_A(z, r)$. A fixed point of the set of equations is known as the self-consistent-field (SCF) solution. Once the SCF solution is known, the partition function can be considered to be optimized and the grand potential Ω can be evaluated. The grand potential can be written as²⁰

$$\frac{\Omega}{k_B T} = - \sum_z \sum_r L(r) \Pi(z, r) \quad (15)$$

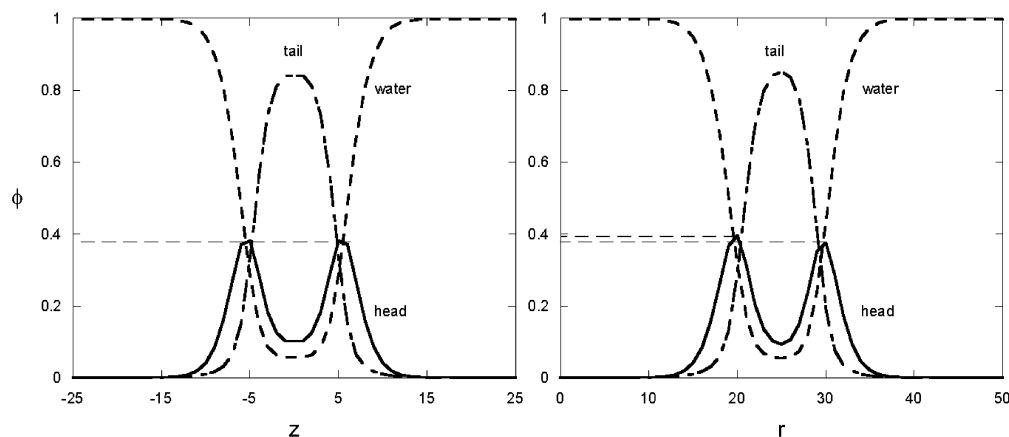


Figure 3. Density profiles of tails, heads, and solvent group of the torus from C₁₀E₄ surfactants. The profiles are across the center of the cross section of the torus in the orthogonal direction z (left) and radial direction r (right). In this torus the aggregation number $n^s = 408$, which corresponds to radius of the torus $R_t \approx 25.2$ and $\phi^b = 0.003$. The default parameter set is used.

where $\Pi(z, r)$ is known as the dimensionless grand potential density,

$$\Pi(z, r) = \sum_A \phi_A(z, r) \frac{u_A(z, r)}{k_B T} + \sum_i \left(\frac{\phi_i(z, r)}{N_i} - \frac{n_i}{G_i(1|N)} \right) - \frac{1}{2} \sum_A \sum_B \chi_{AB} \{ \phi_A(z, r) (\langle \phi_B(z, r) \rangle - \phi_B^b) - \phi_A^b (\phi_B(z, r) - \phi_B^b) \} \quad (16)$$

where $\phi_i(z, r) = \sum_s \phi_i(z, r, s)$ gives the overall density of molecule i at coordinate (z, r) .

3. Model Parameters

As discussed above, to determine the equilibrium distribution of chain molecules by using this model, the primary sequence of segment of the chains, the geometry of the lattice, the Flory–Huggins interaction parameters, and the number of molecules in the system are needed as input parameters.

Our calculations are carried out for nonionic surfactants C_{*n*}(OC₂)_{*m*}O, abbreviated as C_{*n*}E_{*m*}. Here, C refers to CH₂ or CH₃ groups and O refers to oxygen or hydroxyl groups. The water molecules are modeled as dimers W₂. Correspondingly, a set of three Flory–Huggins interaction parameters χ_{CO} , χ_{CW} , and χ_{OW} are used. The value of χ_{CO} must reflect a repulsive interaction between the hydrophobic tail and the hydrophilic headgroups (here $\chi_{CO} = 2.2$ is used). The value of χ_{CW} indicates hydrophobicity of the tail groups ($\chi_{CW} = 1.4$) and the value of χ_{OW} is related to the hydrophilicity of the headgroups. A default value of $\chi_{OW} = -0.5$ is used. To estimate the temperature dependence of the bending moduli, we follow previous work²³ using the Ansatz $\chi_{OW} \sim T^{-1}$ and keep all other interaction parameters constant. As a result, the surfactant headgroup becomes less polar with increasing temperature. This is in line with experimental data on the critical micellization temperature (CMT) and cloud point temperature of EO-based surfactant solutions.²³

The area per molecule a_0 of surfactants in the micelle is, to first order, a preserved quantity. Also, the equilibrium concentration of surfactants floating free in solution is almost constant (above CMC). This means that the total number of surfactants in the system sets the total length of the wormlike micelle. This quantity also sets the radius of the torus.

All calculations are performed in a cylindrical coordinate system with dimensions that are at least $2M_z = M_r = 40$. In all

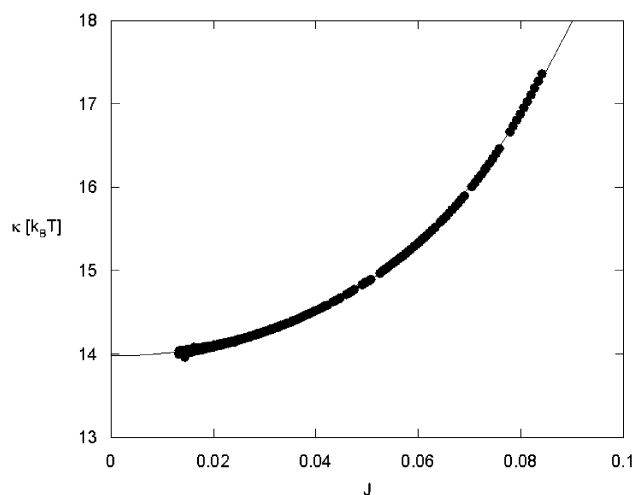


Figure 4. The bending modulus κ of a cylindrical micelle as a function of curvature J for C₁₀E₄. The extrapolation of κ to $J = 0$ is made from this plot. $\kappa(0)$ is interpreted as the bending modulus of the torus in the Helfrich eq 2.

cases the system size is set large enough such that the densities attain bulk values before reaching the system boundaries.

4. Results and Discussions

An example of the density profile of a torus predicted from the SCF calculation is depicted in Figure 3. It is the torus for C₁₀E₄, with aggregation number (total number of surfactant molecules for each torus) $n^s = 408$ and volume fraction of free surfactant molecules in the solution $\phi^b = 0.003$. The corresponding radius of the torus $R_t \approx 25.2$ (in units of the length of a lattice site). In this work, $J = 1/R_t$ is estimated from the ratio between the excess number of surfactant (aggregation number) of the torus, n^s , to the aggregation number per unit length of a straight wormlike micelle n_0^s that is calculated in the limit $J \rightarrow 0$, i.e., $J = 2\pi(n_0^s)/(n^s)$. Another way to compute J is from the first moment of the excess radial density distribution of the surfactant molecules, as depicted in Figure 3.

The density profiles in Figure 3 result from a cut through the center of the cross-section of the torus in the orthogonal direction (left figure) and radial direction (right figure). The density of the hydrophilic head groups is maximum near the water–surfactant interface of the torus (known as corona), the density of hydrophobic tail groups is maximum in the center of the cross-section. A low-volume fraction of solvent is present in the core of the torus and becomes almost unity in the bulk.

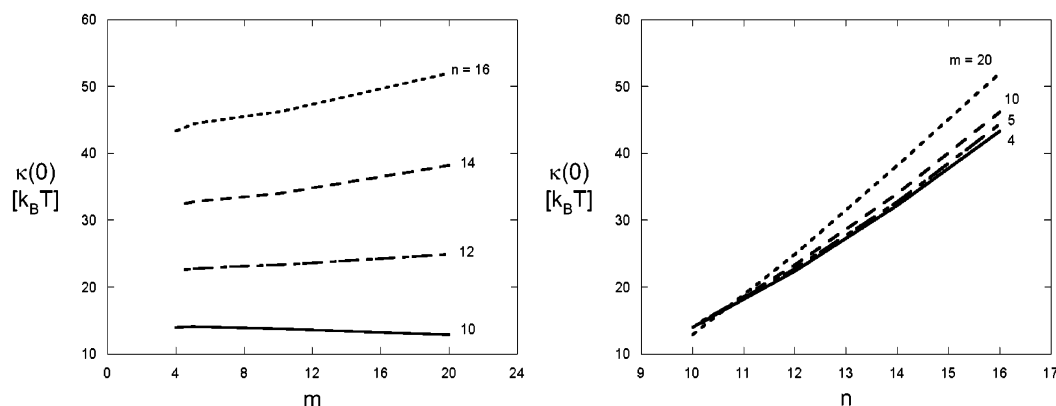


Figure 5. The bending moduli κ of cylindrical micelles at zero curvature $\kappa(0)$ of C_nE_m surfactants. The left figure shows the effect of head group length m , and the right figure shows the effect of the tail length n .

It can be seen that in the orthogonal direction, the profiles of the head and tail groups, as well as that of the solvent are symmetrical. As expected, profiles in the radial direction are not symmetrical, the headgroups being packed more densely at the inner part of the torus than on the outer part due to the difference in curvature on both sides. This is easily understood since at the inner part, the headgroups have less space than at the outer part, which leads to a higher packing density. The tails, on the other hand, have their highest density on the outer half of the torus ($r > 25$). These asymmetries in the profiles are the locus where curvature energy is stored.

From the SCF calculations in the cylindrical coordinate system, it is possible to evaluate the persistence length directly from the grand potential Ω (eq 4) once the curvature J is known. Indeed, our procedure allows us to evaluate $\Omega(J)$ and thus enables us to evaluate the persistence length as a function of J . An example of such a result is presented in Figure 4. In this figure it is seen that κ is an increasing function of J .

Since the Helfrich equation is only valid for infinitesimal values of J , the extrapolation of the curve to $J = 0$ gives the value of bending modulus κ applicable in eq 2. We first analyze $\kappa(0)$ and return afterward to the curvature dependence of the bending modulus. In this article, the persistence length l_p is obtained from $\kappa(0)$ based on eq 1. As shown in Figure 5, the limiting bending modulus $\kappa(0)$ is a weak function of the headgroup length m but a strongly increasing function of the tail group length n . In this figure we use a relevant range of n and m values. Obviously, cylindrical micelles are expected only for specific combinations of n and m . The fact that the persistence length is just a weak function of m allows us to predict that the persistence length of a wormlike micelle is given by the length of the tail group only. It is necessary to mention that our calculations do not prove that cylindrical micelles exist for all combinations of n and m . It may well be that spherical micelles are preferred for relatively large m or bilayers are more likely for large n . However, here the torus is put as a constraint. The persistence length l_p scales with the tail group length n of the surfactant as $l_p \sim n^x$ where x is about 2.4–2.9. This is in line with results for bilayers.

The bending properties of bilayers have received some attention in the literature.^{21,24–25} It is known that the bending modulus of a surfactant layer is a weak function of the hydrophilic part and strongly depends on the hydrophobic part. For bilayers with fixed area per molecule, the bending modulus κ scales with the hydrophobic chain length n as $\kappa \sim n^x$ where $x \approx 2.5$.²⁶

In general, we should expect that the rigidity of a wormlike micelle increases both with the size of the core as well as with

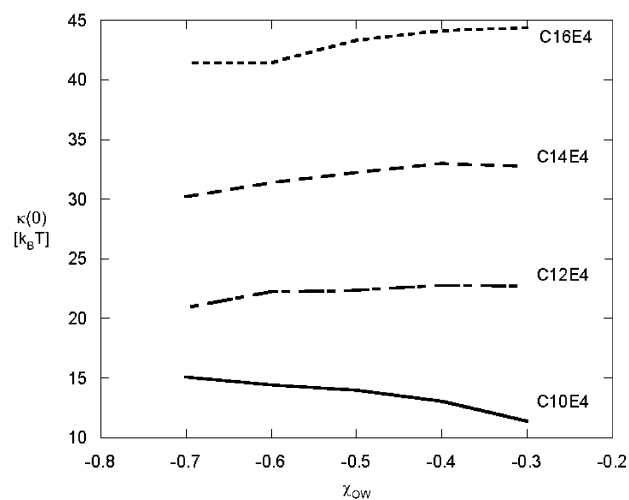


Figure 6. The bending modulus of a cylindrical micelle as a function of hydrophilicity of the headgroup for various surfactants as indicated.

that of the corona. The wormlike micelles are more rigid when the surfactants contain more hydrophobic groups. This is obvious because the core size will increase with the length of the tail (at fixed headgroup size). The insignificance of the headgroup size to the persistence length is due to the compensation of two opposite effects: at fixed tail length, increasing m enlarges the corona but reduces the core size. A larger corona typically increases the bending rigidity, but a small core decreases it. Apparently, these two effects largely cancel.

Changing the hydrophilicity of the headgroup of surfactants does not lead to large changes in bending modulus as can be seen in Figure 6. The decrease in hydrophilicity can be interpreted as an increase in temperature T since $\chi \sim T^{-1}$. For a short tail group, the increase in temperature causes a decrease in bending modulus. However, for reasonably longer tail groups, an increase in temperature leads to the opposite effect, i.e., the torus becomes more rigid with increasing temperature.

So far, we only discussed the bending rigidity in the limit of $J \rightarrow 0$. For a larger curvature, both the bending modulus and the persistence length are functions of the curvature (Figure 4) and in general they must be specified as $\kappa(J)$ or $l_p(J)$. It turns out that the grand potential $\Omega(J)$, and thus, $\kappa(J)$ and $l_p(J)$ can always be fitted to a polynomial function of J of even degree. This is not a surprise, since for symmetry reasons the surface bending should not depend on the sign of J . We find that it is necessary to include J^4 and J^6 terms to be able to fit $\Omega(J)$ over the whole range of J . Therefore, $\kappa(J)$ becomes available up to order J^4 .

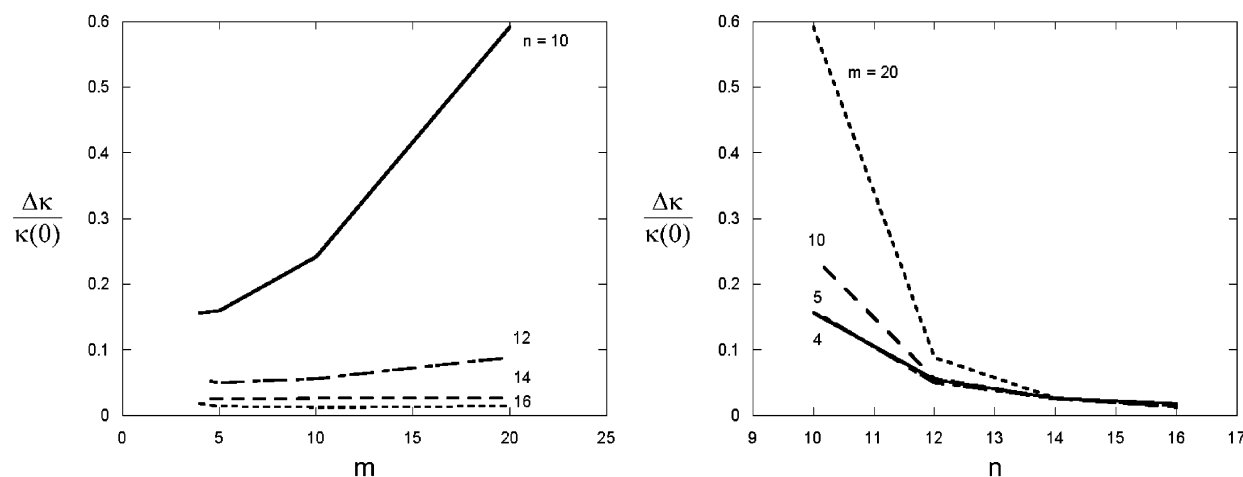


Figure 7. The normalized difference of bending moduli of a cylindrical micelle $\Delta\kappa/\kappa(0)$ as a function of the headgroup length m (left) and tail group length n (right) for various values of m and n respectively as indicated.

The Helfrich eq 2 for the torus is extended accordingly and written as

$$\frac{\Omega}{l} = \frac{1}{2}\kappa J^2 + \frac{1}{4!}\kappa' J^4 + \frac{1}{6!}\kappa'' J^6 \equiv \frac{1}{2}\kappa(J)J^2 \quad (17)$$

where

$$\kappa(J) = \kappa + \frac{2}{4!}\kappa' J^2 + \frac{2}{6!}\kappa'' J^4 \quad (18)$$

where $\kappa = \kappa(0)$ is the bending modulus of the torus in the original Helfrich eq 2 already discussed above; κ' and κ'' are the coefficients that correspond to the higher order terms of the bending modulus.

The significance of the higher order terms of the bending modulus can be seen in Figure 7. In this figure, we present the difference $\Delta\kappa$ between the bending moduli at the curvature equal to the inverse persistence length ($R_t = l_p$) and at zero curvature ($R_t \rightarrow \infty$), normalized to the bending modulus at zero curvature as follows:

$$\frac{\Delta\kappa}{\kappa(0)} = \frac{\kappa(l_p^{-1})}{\kappa(0)} - 1 \quad (19)$$

This quantity is plotted in Figure 7 as a function of the headgroup length m and tail group length n . It turns out that the higher order terms of the bending modulus at curvatures of the order of the inverse persistence length are more pronounced for surfactants with a relatively large headgroup and a small tail group. This indicates that the hydrated corona, which is relatively unimportant for $\kappa(0)$, does extend significantly into solution and then influences the stiffness of the wormlike micelles especially at high curvatures.

5. Concluding Remarks and Outlook

The persistence length is an important parameter in describing the flexibility/rigidity of wormlike micelles. This parameter is typically treated phenomenologically. We have shown that it is possible to calculate the persistence length of wormlike micelles by means of a numerical SCF theory that accounts for molecular details. The bending rigidity, or equivalently, the persistence length, of wormlike micelles follows unambiguously from a Helfrich-like (up to second order) expansion of the grand potential of toroidal micelles in terms of the (small) curvature J . As a result, we can propose a molecular interpretation of this

quantity. It was found that the bending rigidity of wormlike micelles is only a function of the tail length n of the surfactant. The independence of the rigidity of the micelle on the headgroup size is caused by the cancellation of two opposing effects: a large corona reduces the core size. This means that both the dimension of the core as well as that of the corona affect the flexibility of the wormlike micelle.

Quantitatively, the persistence length l_p scales with the tail group length of the surfactant as $l_p \sim n^x$ where x is about 2.4–2.9. This is expected since the core size increases almost linearly with n (at fixed m). The rather high value of the exponent ($x > 2$) may be due to the fact that the average density of the tail group in the hydrophobic core of the micelle increases slightly with the tail length n .

For larger curvatures, already for radii of curvature in the order of inverse persistence length ($R_t \leq l_p$), higher order terms of bending modulus become important. As a result, we find that the persistence length is a function of the curvature. The higher order contributions to the bending modulus are more important for surfactants with a relatively large hydrophilic headgroup. This may be attributed to curvature-dependent steric interactions between the headgroups in highly curved parts of the wormlike micelle.

In the future we plan to use the same SCF procedure to obtain corresponding results for wormlike micelles composed of ionic surfactants.

Acknowledgment. Part of this work was supported by STW grant EPC.5516.

References and Notes

- (1) Van de Sande, W.; Persoons, A. *J. Phys. Chem.* **1985**, *89*, 404.
- (2) Cates, M. E.; Candau, S. J. *J. Phys. Condens. Matter* **1990**, *2*, 6869.
- (3) Den Otter, W. K.; Shkulipa, S. A.; Briels, W. J. *J. Chem. Phys.* **2003**, *119*, 2363.
- (4) Israelachvili, J. N.; Mitchell, D. J.; Ninham, B. W. *J. Chem. Soc., Faraday Trans. 2* **1976**, *72*, 1525.
- (5) Porte, G. In *Micelles, Membranes, Microemulsions and Monolayers*; Gelbart, W. M., Ben-Shaul, A., Roux, D., Eds.; Springer: Berlin, 1994; Chapter 2.
- (6) Lin, Z.; Cai, J. J.; Scriven, L. E.; Davis, H. T. *J. Phys. Chem.* **1994**, *98*, 5984.
- (7) Porte, G.; Appell, J.; Poggi, Y. *J. Phys. Chem.* **1980**, *84*, 3105.
- (8) Porte, G. *J. Phys. Chem.* **1983**, *87*, 3541.
- (9) Lin, Z.; Scriven, L. E.; Davis, H. T. *Langmuir* **1992**, *8*, 2200.
- (10) Cohen, D. E.; Thurston, G. M.; Chamberlin, R. A.; Benedek, G. B.; Carey, M. C. *Biochemistry* **1998**, *37*, 14798.
- (11) Bernheim-Groszasser, A.; Zana, R.; Talmon, Y. *J. Phys. Chem. B* **2000**, *104*, 12192.
- (12) In, M.; Aguerre-Chariol, O.; Zana, R. *J. Phys. Chem. B* **1999**, *103*, 7747.

- (13) Clausen, T. M.; Vinson, P. K.; Minter, J. R.; Davis, H. T.; Talmon, Y.; Miller, W. G. *J. Phys. Chem.* **1992**, 96, 474.
- (14) Lifshitz, E. M.; Pitaevskii, L. P. *Statistical Physics*, 3rd ed.; Pergamon Press: Oxford, 1980; Vol. 5, Part 1, p 127.
- (15) Helfrich, W. Z. *Naturforsch. C* **1973**, 28c, 693.
- (16) Scheutjens, J. M. H. M.; Fleer, G. J. *J. Phys. Chem.* **1979**, 83 (12), 1619.
- (17) Scheutjens, J. M. H. M.; Fleer, G. J. *J. Phys. Chem.* **1980**, 84 (2), 178.
- (18) Leermakers, F. A. M.; Scheutjens, J. M. H. M. *J. Chem. Phys.* **1988**, 89 (5), 3264.
- (19) Leermakers, F. A. M.; Scheutjens, J. M. H. M. *J. Phys. Chem.* **1989**, 93 (21), 7417.
- (20) Evers, O. A.; Scheutjens, J. M. H. M.; Fleer, G. J. *Macromolecules* **1990**, 23, 5221.
- (21) Oversteegen, S. M.; Leermakers, F. A. M. *Phys. Rev. E* **2000**, 62, 8453.
- (22) Van der Schoot, P. P. A. M.; Leermakers, F. A. M. *Macromolecules* **1988**, 21, 1876.
- (23) De Bruijn, V. G.; Van den Broeke, L. J. P.; Leermakers, F. A. M.; Keurentjes, J. T. F. *Langmuir* **2002**, 18, 10467.
- (24) May, S.; Bohbot, Y.; Ben-Shaul, A. *J. Phys. Chem. B* **1997**, 101, 8648.
- (25) Ennis, J. J. *J. Chem. Phys.* **1992**, 97, 663.
- (26) Szleifer, I.; Kramer, D.; Ben-Shaul, A. *Phys. Rev. Lett.* **1988**, 60 (19), 1966.